THERMOMECHANICAL ANALYSIS OF VEHICLE BRAKING

Ali BELHOCINE[1], Mostefa BOUCHETARA[2]

The main purpose of this study is to analyze the thermomechanical behavior of the dry contact between the brake disc and pads during the braking phase. The simulation strategy is based on computer code ANSYS11. The modeling of transient temperature in the disc is actually used to identify the factor of geometric design of the disc to install the ventilation system in vehicles. The thermal-structural analysis is then used with coupling to determine the deformation and the Von Mises stress established in the disc, the contact pressure distribution in pads. The results are satisfactory when compared to those of the specialized literature.

Keywords: Brake discs, Heat flux, Heat-transfer coefficient, Von Mises stress, Contact pressure

1. Introduction

The braking process is a fact the matter of energy balance. The aim of braking system is to transform mechanical energy of moving vehicle into some other form, which results in decreasing the speed of the vehicle. The kinetic energy is transformed into the thermal energy by means of the dry friction effects, which then is dissipated into the surroundings [1].

Ventilated disc-pad brakes (Fig. 1) are widely used for reducing velocity due to their braking stability, controllability and ability to provide a wide-ranging brake torque. The brake disc with vanes rotates through the caliper. A ventilated disc with straight vanes is most popular, easy and straightforward to make.

In the study conducted by Voloacă and Frătilă [2], an analysis of thermal stress which appears in two different brake discs, with different geometries was presented.

In this study, we will make a modeling of the thermomechanical behavior of the dry contact between the discs of brake pads at the time of braking phase; the strategy of calculation is base on the software ANSYS 11 [3].

[1] PhD Student., Dept.of Mech Eng, USTO Oran University,Algeria, e-mail: al.belhocine@yahoo.fr
[2] Prof., Dept.of Mech Eng, USTO Oran University , Algeria, e-mail: mbouchetara@hotmail.com

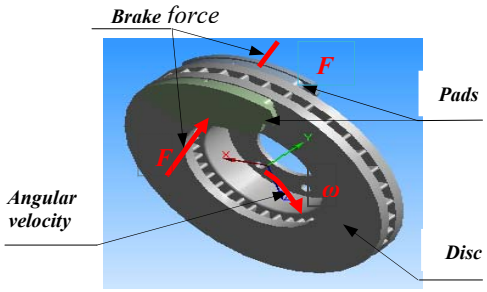

Fig.1. Disc-pads assembly with forces applied to the disc

2. Heat flux entering the disc

In the case of disc brake, the effective friction processes between the pads and the disc are extremely complex because the present time brake pads, due to their composite structure [4], do not have constant chemical-physical properties, with the organic containing elements being subjected to a series of transformations under the influence of temperature increase. The geometrical characteristics of the ventilated disc are illustrated in Fig.2. The brake disc consumes the major part of the heat, usually greater than 90% [5], by means of the effective contact surface of the friction coupling. Considering the complexity of the problem and the limitation in the average data processing, one identifies the pads by their effect, represented by an entering heat flux (Fig.3).

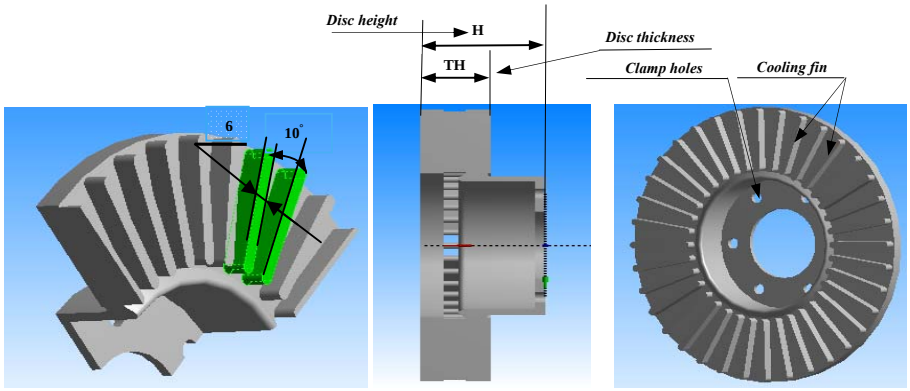

Fig.2. Geometrical characteristics of the ventilated disc

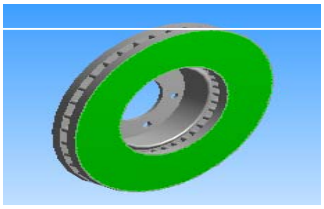

Fig.3. Application of flux

The initial heat flux q_0 entering the disc is calculated by the following formula [6]:

$$q_0 = \frac{1-\phi}{2} \cdot \frac{mgv_0 z}{2A_d \varepsilon_p} \quad [kg/s^3] \tag{1}$$

where $z = a/g$ is the braking effectiveness, a is the deceleration of the vehicle [m/s^2], ϕ is the rate distribution of the braking forces between the front and rear axle, A_d disc surface swept by a brake pad [m^2], v_0 is the initial speed of the vehicle [m/s], ε_p is the factor load distribution on the surface of the disc., m is the mass of the vehicle [kg] and g is the acceleration of gravity (9.81) [m/s^2].

The loading corresponds to the heat flux on the disc surface. The dimensions and the parameters used in the thermal calculation are recapitulated in Table 1.

The disc material is gray cast iron (GFC) with high carbon content [7], with good thermophysical characteristics and the brake pad has an isotropic elastic behavior, whose thermomechanical characteristics adopted in this simulation of the two parts are listed in Tab 2.

Table 1. Parameters of automotive brake application

Inner disc diameter, mm	66
Outer disc diameter, mm	262
Disc thickness (TH) ,mm	29
Disc height (H) ,mm	51
Vehicle mass m , kg	1385
Initial speed v_0 , m/s	28
Deceleration a , m/s^2	8
Effective rotor radius R_{rotor} ,mm	100.5
Rate distribution of the braking forces ϕ, %	20
Factor of charge distribution of the disc ε_p	0.5
Surface disc swept by the pad A_d , mm^2	35993

To simplify the analysis, several assumptions have also been made as follows [8]:

- All kinetic energy at disc brake rotor surface is converted into frictional heat or heat flux.
- The heat transfer involved for this analysis is only conduction and convection processes. This heat transfer radiation can be neglected in the analysis because of itssmall amount which is 5% to 10% [9].
- The disc material is considered as homogeneous and isotropic.

- The domain is considered as axis-symmetric.
- Inertia and body force effects are negligible during the analysis.
- The disc is stress free before the application of brake.
- In this analysis, the ambient temperature and initial temperature have been set to 20°C
- All other possible disc brake loads are neglected.
- Only certain parts of disc brake rotor will apply with convection heat transfer such as cooling vanes area, outer ring diameter area and disc brake surface
- Uniform pressure distribution is applied by the brake pad onto the disc brake surface.

The thermal conductivity and specific heat are a function of temperature, Figures 4 and 5.

Table 2.Thermoelastic properties used in simulation

Material Properties	Pad	Disc
Thermal conductivity, k (W/m°C)	5	57
Density, ρ (kg/m^3)	1400	7250
Specific heat, C_p (J/Kg °C)	1000	460
Poisson's ratio, ν	0.25	0.28
Thermal expansion, α (10^{-6} / °C)	10	10.85
Elastic modulus, E (GPa)	1	138
Coefficient of friction, μ	0,2	0,2
Operation Conditions		
Angular velocity, ω (rad/s)		157.89
Hydraulic pressure, P (MPa)		1

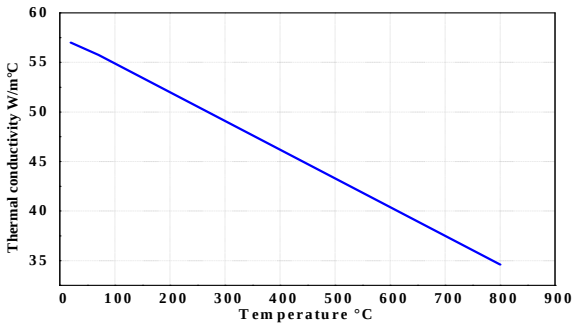

Fig.4. Thermal conductivity versus temperature

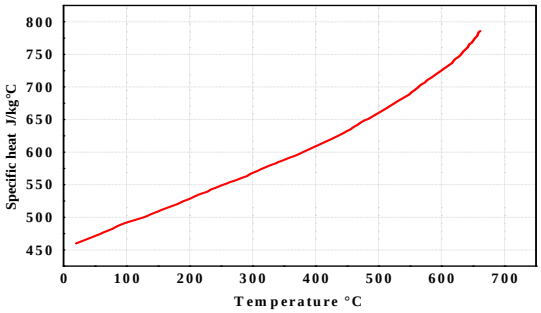

Fig.5. Specific heat versus temperature

3 Numerical modeling of the thermal problem

3.1 Equation of the problem

The first law of thermodynamics indicating the thermal conservation of energy gives:

$$\rho C_p\left(\frac{\partial T}{\partial t}+\{v\}^T\{L\}T\right)+\{L\}^T\{Q\}=p \tag{2}$$

In our case there is not an internal source $(p=0)$, thus equation (2) is written:

$$\rho C_p\left(\frac{\partial T}{\partial t}+\{v\}^T\{L\}T\right)+\{L\}^T\{Q\}=0 \tag{3}$$

with:

$$\{L\}=\begin{Bmatrix}\dfrac{\partial}{\partial x}\\ \dfrac{\partial}{\partial y}\\ \dfrac{\partial}{\partial z}\end{Bmatrix} \tag{4}$$ and $$\{v\}=\begin{Bmatrix}v_x\\ v_y\\ v_z\end{Bmatrix} \tag{5}$$

Fourier's law (3) can be written in the following matrix form:

$$\{Q\}=-[K]\{L\}T \tag{6}$$

with:

$$[K]=\begin{bmatrix}k_{xx} & 0 & 0\\ 0 & k_{yy} & 0\\ 0 & 0 & k_{zz}\end{bmatrix} \tag{7}$$

k_x, k_y and k_z represent the thermal conductivity along axes x, y, z respectively. In our case the material is isotropic thus $k_{xx}=k_{yy}=k_{zz}$

- $\{L\}$ Vector operator.
- $\{v\}$ Vector speed of mass transport.
- $[K]$ Conductivity matrix.

By combining two equations (3) and (6), we obtain:

$$\rho C_p\left(\frac{\partial T}{\partial t}+\{v\}^T\{L\}T\right)=\{L\}^T([K]\{L\}T) \tag{8}$$

By developing equation (8) we obtain: $\rho C_p\left(\frac{\partial T}{\partial t}+v_x\frac{\partial T}{\partial x}+v_y\frac{\partial T}{\partial y}+v_z\frac{\partial T}{\partial z}\right)$

$$=\frac{\partial}{\partial x}\left(k_x\frac{\partial T}{\partial x}\right)+\frac{\partial}{\partial y}\left(k_y\frac{\partial T}{\partial y}\right)+\frac{\partial}{\partial z}\left(k_z\frac{\partial T}{\partial z}\right) \tag{9}$$

3.2 Initial Conditions

We suppose that the initial temperature of the disc is constant.

$$T(x,y,z)=60°C \quad \text{at time} \quad t=0 \tag{10}$$

3.3 Boundary conditions

In general, in a thermal study, one finds three types of boundary conditions:

1. Temperature specified on a surface

$$S_T : T=T^* \tag{11}$$

2. Heat flux specified on a surface

$$S_Q : \{Q\}^T\{n\}=-Q^* \tag{12}$$

3. Convection specified on a surface

$$S_C : \{Q\}^T\{n\}=h(T_p-T_f) \tag{13}$$

3.4. Preparation of the Mesh

This stage consists in preparing the mesh of the fluid field. In our case, one used a linear tetrahedral element with 30717 nodes and 179798 elements (Fig.6).

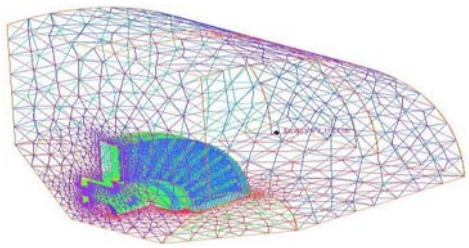

Fig.6. Mesh of the fluid field.

4. Modeling in ANSYS CFX

The solution scheme employees the κ-ε model with scalable wall function and sequential load steps. For the preparation of the mesh of CFD model, one defines initially various surfaces of the disc in ICEM CFD as shown in Fig 7 and Fig.8; we used a linear tetrahedral element;the mesh contained 30717 nodes and 179798 elements. In order not to weigh down calculation, an irregular mesh is used in which the mesh is broader where the gradients are weaker (nonuniform mesh) (Fig.9).

The CFD models were constructed and were solved using ANSYS-CFX software package [10]. The model applies periodic boundary conditions on the section sides. As the brake disc is made from sand-casted grey cast iron, the disc model is attached to an adiabatic shaft whose axial length spans that domain. Air around the disc is considered to be 20 °C and open boundaries with zero relative pressure were used for the upper, lower and radial ends of the domain. Material data was taken from the ANSYS material data library for air at 20 °C. Reference pressure was set to be 1 atm, low turbulence intensity and the turbulent model used was k-ε. (Fig.10)

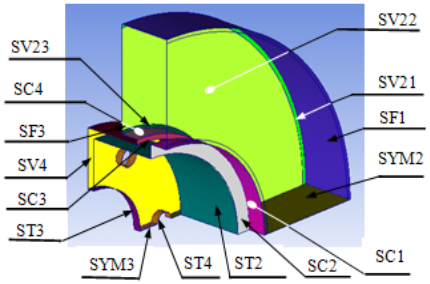

Fig.7. Definition of surfaces of the full disc

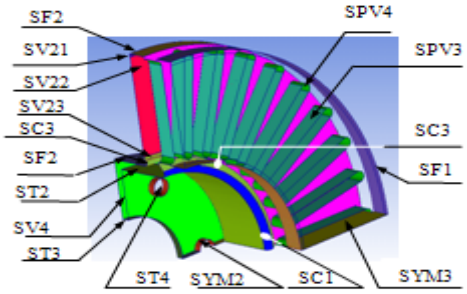

Fig.8. Definition of surfaces of the ventilated disc

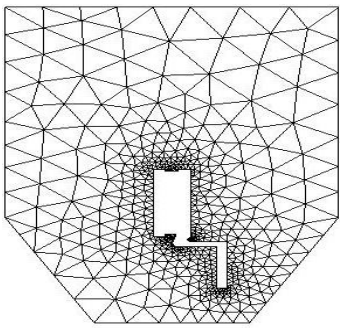

Fig.9. Irregular mesh in the wall

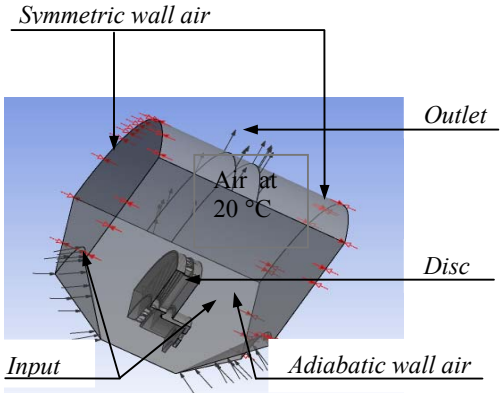

Fig.10. Brake disc CFD model

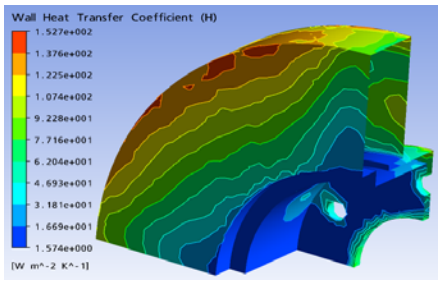

Fig.11.Distribution of heat transfer coefficient on a full disc in the steady state case (FG 15)

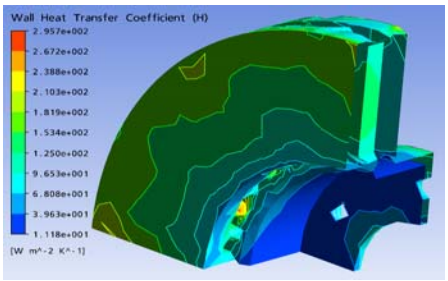

Fig.12.Distribution of heat-transfer coefficient on a ventilated disc in the stationary case (FG 15).

The airflow through and around the brake disc was analyzed using the ANSYS-CFX software package. The ANSYS-CFX solver automatically calculates heat-transfer coefficient at the wall boundary. Afterwards the heat-transfer coefficients considering convection were calculated and organized in such a way, that they could be used as a boundary condition in thermal analysis. Averaged heat-transfer coefficient had to be calculated for all disc using ANSYS-CFX Post as it is indicated in Figs.11. and 12.

a) Results of the calculation of the heat-transfer coefficient (h)

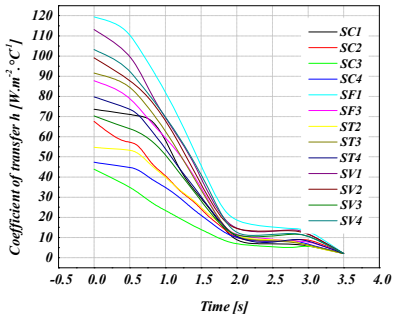

Fig.13.Variation of heat-transfer coefficient *(h)* of various surfaces for a full disc in the nonstationary case (FG 15)

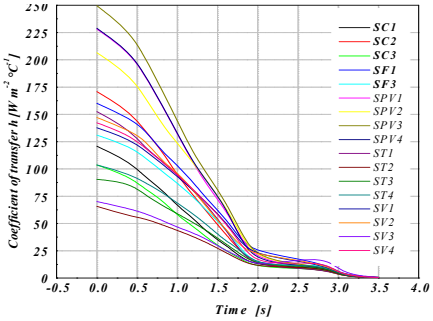

Fig.14.Variation of heat-transfer coefficient *(h)* of various surfaces for a ventilated disc in transient case (FG 15)

From the comparison between Figs. 13 and 14 concerning the variation of heat-transfer coefficients in the nonstationary mode for the two types of design full and ventilated disc, one notes that the introduction of the system of ventilation directly influences the value of this coefficient for the same surface, which is logically significant because this mode of ventilation results in the reduction in the differences in wall-fluid temperatures.

5. Meshing of the disc

The elements used for the mesh of the full and ventilated disc are tetrahedral 3D elements with 10 nodes (isoparametric) (Fig.15).

(a) full disc (172103 nodes -114421 elements) (b) ventilated disc(154679 nodes- 94117 elements)
Fig.15. Meshing of the disc

6. Initial and boundary conditions

The boundary conditions are introduced into module ANSYS Workbench [Multiphysics], by choosing the mode of first simulation of the all (permanent or transitory) and by defining the physical properties of materials. These conditions constitute the initial conditions of our simulation. After having fixed these parameters, one introduces a boundary condition associated with each surface.

- Total time of simulation = 45 [s]
- Increment of initial time = 0.25 [s]
- Increment of minimum initial time = 0.125 [s]
- Increment of maximum initial time = 0.5 [s]
- Initial Temperature of the disc = 60 [°C]
- Materials: Gray Cast iron FG 15.
- Convection: One introduces the values of the heat-transfer coefficient *(h)* obtained for each surface in the shape of a curve.
- Flux: One introduces the values obtained by flux entering by means of the code CFX.

6. Influence of construction of the disc

Fig.16 shows the variation of the temperature versus time during the total time simulation of braking for a fall disc and a ventilated disc. The highest temperatures are reached at the contact surface of disc-pads. The strong increase in temperature is due to the short duration of the braking phase and to the speed of the physical phenomenon. For the two types of discs, one disc has an immediate, fast temperature increase followed by a fall in temperature after a certain time of braking.

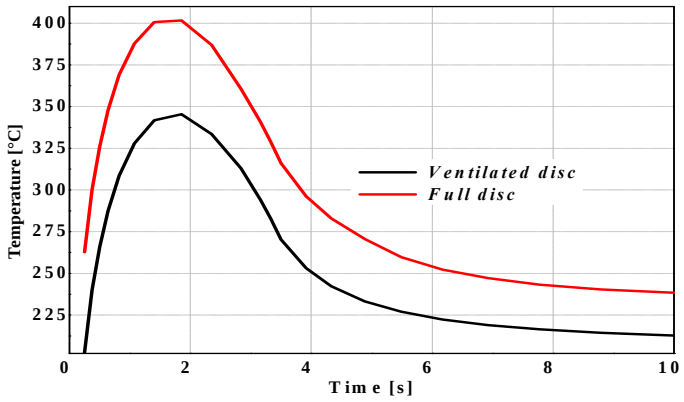

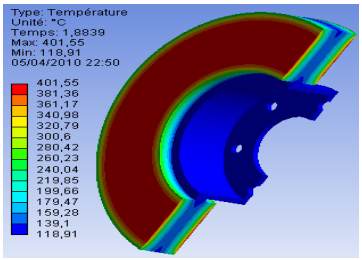

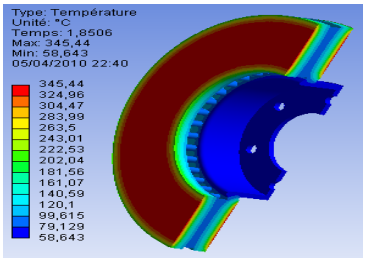

(a) (b)

Fig.16. Temperature distribution of a full (a) and ventilated disc (b) of cast iron (FG 15)

For the full disc, the temperature reaches its maximum value of 401.55 °C at the moment t = 1.8839 s and then it falls rapidly to 4.9293 s as from this moment and to the end (t = 45 s) of simulation, the variation in the temperature becomes slow. It is noted that the interval [0-3.5] s represents the phase of forced convection. During this phase, one observes the case of the free convection until the end of the simulation. In the case of the ventilated disc, one observes that the temperature of the disc falls approximately by 60 °C compared with the first case. It is noted that ventilation in the design of the discs of brake plays an important role in producing a better system of cooling.

7. Coupled Thermomechanical Analysis

Disc brakes operate by pressing a set of brake pads against a rotating brake disc; the frictional forces cause deceleration. The generated dissipation of the frictional heat is critical for effective braking performance. Temperature changes of the brake cause axial and radial deformation and this change in shape; in turn, it affects the contact between the pads and the disc. Thus, the system should be analyzed as a fully coupled thermomechanical system.

7.1. FE model and boundary conditions

Fig.17 shows the FE model and boundary conditions embedded configurations of the model composed of a disc and two pads.

A fully coupled thermomechanical model was set up to predict the temperature changes of the brake disc shape caused by axial and radial deformation. Thermal conduction and convective heat transfer were the two considered modes of heat transfer. The convection heat transfer coefficient has values form the curves of Figure 14 over all exposed surfaces of the disc and radiative heat transfer was considered negligible [11].

The initial air temperature of the disc and pads is 20℃. The surface convection condition is applied at all surfaces of the disc and the convection coefficient *(h)* of 5 W/m^2°C is applied to the surfaces of the two pads. The FE mesh is generated using 3D tetrahedral element with 10 nodes (solid 187) for the disc and pads. Overall, 185901 nodes and 113367 elements are used (Fig.18).

A frictional contact pair was defined between disc-pad interfaces. The used element types were Quadratic Triangular Contact (Conta174) and Quadratic Triangular Target (Target 170). The mechanical properties of the most common disc brakes (grey cast iron) and pad materials used in the analysis are given in Table 2.

In this study, a transient thermal analysis was carried out to investigate the temperature variation across the disc using ANSYS software. Further structural analysis will also be carried out by coupling thermal analysis.

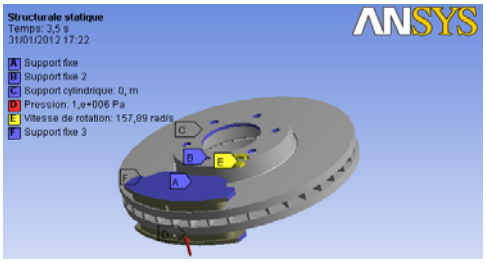

Fig.17. Boundary conditions and loading imposed on the disc-pads

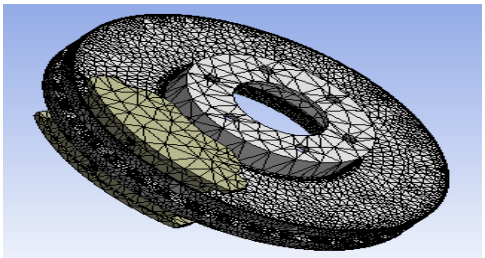

Fig.18. Refined mesh of the model

7.2. Thermal deformation

Fig.19. gives the distribution of the total distortion in the whole (disc-pads) for various moments of simulation. For this figure, the scale of values of the deformation varies from 0 to 284.55 µm. The value of the maximum displacement recorded during this simulation is at the moment t=3.5 s, which corresponds to the time of braking. One observes a strong distribution which increases with time on the friction tracks and the external crown and the cooling fins of the disc. ndeed,

during a braking moment, the maximum temperature depends almost entirely on the heat storage capacity of disc (on particular tracks of friction); this deformation will generate a lack of symmetry of the disc following the increase of temperature which will cause a deformation in the shape of an umbrella.

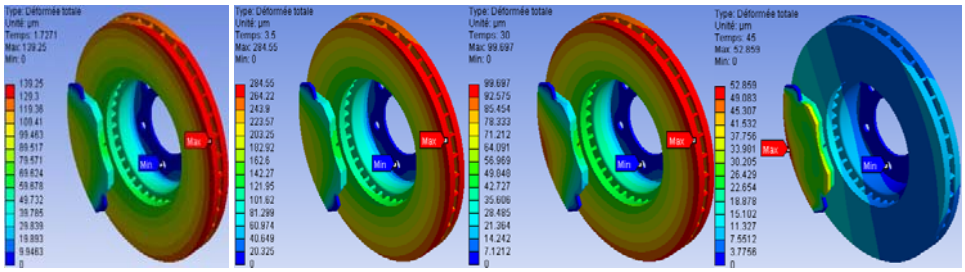

(a) t=1.7271 s (b) t=3.5 s (c) t=30 s (d) t=45 s

Fig.19. Total distortion distribution

7.3. Von Mises stress distribution

Fig.20. presents the distribution of the equivalent Von Mises stress for various moments of simulation, the scale of values varying from 0 to 495.56 MPa. The maximum value recorded during this simulation of the thermomechanical coupling is very significant compared to that obtained with the assistance in the mechanical analysis under the same conditions. One observes a strong constraint on the level of the bowl of the disc. Indeed, the disc is fixed to the hub of the wheel by screws, thus preventing its movement. In the presence of the rotation of the disc and the requests of torsional stress and sheers generated at the level of the bowl which are able to create the stress concentrations. The repetition of these effects will lead to risks of failure on the level of the bowl of the disc.

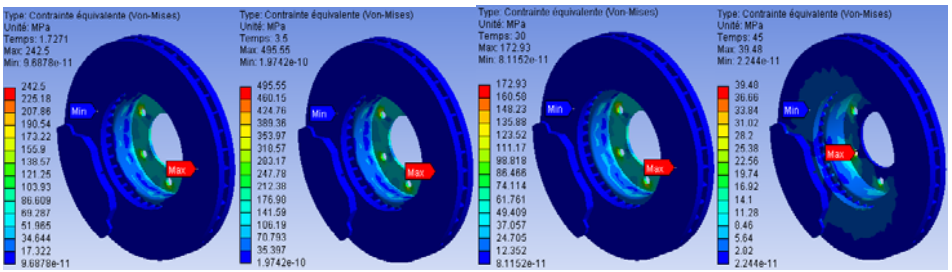

(a) t=1.7271 s (b) t=3.5 s (c) t=30 s (d) t=45 s

Fig.20. Von Mises stress distribution.

7.4. Contact pressure

Fig.21 shows the contact pressure distribution in the friction interface of the inner pad taken at various times of simulation. For this distribution, the scale varies from 0 to 3.3477 MPa and reached a maximum value at the moment t=3.5 s, which corresponds to the null rotational speed. It is also noticed that the maximum contact pressure is located on the edges of the pad decreasing from the leading edge towards the trailing edge from friction. This pressure distribution is almost symmetrical compared with the groove and has the same tendency as that of the distribution of the temperature because the highest area of the pressure is located in the same sectors. Indeed, at the time of the thermomechanical coupling of 3D, the pressure produces the symmetric field of the temperature. This last one affects thermal dilatation and leads to a variation of the contact pressure distribution.

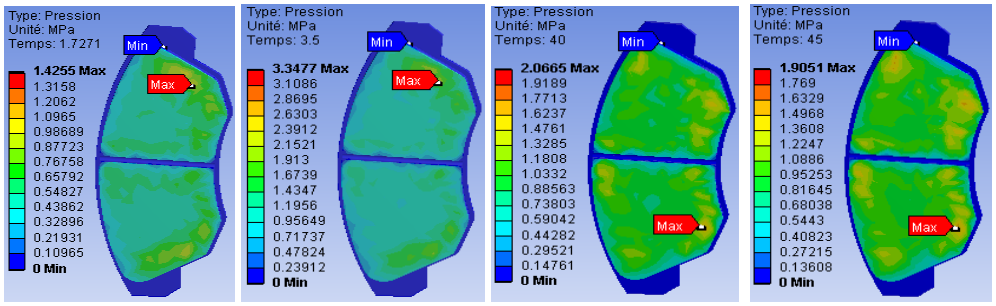

(a) t=1.7271 s (b) t=3.5 s (c) t=40 s (d) t=45 s

Fig.21. Contact pressure distribution in the inner pad

8. Conclusion

In this article, we have presented the analysis of thermomechanical behavior of the dry contact between the brake disc and pads during the braking process; the modeling is based on the ANSYS 11.0. We have shown that the ventilation system plays an important role in cooling the discs and provides a good high-temperature resistance. The analysis it results showed that temperature field and stress field in the process of braking phase were fully coupled. The temperature, Von Mises stress and the total deformations of the disc and contact pressures of the pads increase as the thermal stresses are apart from the mechanical stress which causes the crack propagation and fracture of the bowl and wear of the disc and pads. Regarding the calculation results, we can say that they are satisfactorily in agreement with those commonly found in the literature investigations. It would be interesting to solve the problem in thermo-mechanical disc brakes with an experimental study to validate the numerical results, for

example, on test benches, in order to demonstrate a good agreement between the model and reality.

Regarding the outlook, there are three recommendations for the expansion of future work related to disc brake that can be done to further understand the effects of thermomechanical contact between the disc and pads, as follows:

- Experimental study to verify the accuracy of the numerical model developed.
- Tribological and vibratory study of the contact disc – pads;
- Study of dry contact sliding under the macroscopic aspect (macroscopic state of the surfaces of the disc and pads).

R E F E R E N C E S

[1]. *H.Belghazi*, Analytical Solution of unsteady Heat Conduction in a Two - Layered Material in Imperfect Contact Subjected to a Moving Heat Source, PhD Thesis, University of Limoges, 2010.

[2].*Ş.Voloacă, G.Frăţilă*, Concerns Regarding Temperature Distribution Obtained by Experiments and Finite Element Analyses for Two Types of Brake Discs, U.P.B. Sci. Bull., Series D, Vol. 74, Iss. 3, 2012 pp 34-42.

[3] *Lele Zhang, Qiang Yang, D Weichert , Nanlin Tan*, Simulation and Analysis of Thermal Fatigue Based on Imperfection Model of Brake Discs, Beijing Jiaotong University , PAMM Proc. Appl. Math. Mech. 9, 533 – 534 ,2009.

[4]. ******Fiche U.I.C .541-3*, FREIN – Frein à disques et garnitures de frein à disques, 4e édition, 1 July, 1993.

[5].*C. Cruceanu ,* Frâne Pentru Vehicule Feroviare (Brakes for Railway Vehicles , Ed. MATRIXROM, Bucureşti, ISBN 978- 973-755-200-6, 388 pag, 2007.

[6]. *J. Reimpel ,* Technologie de freinage. Vogel Verlag, Würzburg, 1998.

[7]. *P., F., Gotowicki, V., Nigrelli, G., V., Mariotti,* Numerical And Experimental Analysis Of A Pegs-Wing Ventilated Disk Brake Rotor, With Pads And Cylinders, 10th EAEC European Automotive Congress – Paper EAEC05YU-AS04, 2005 Belgrade;

[[8]*M. K. Khalid, M. R. Mansor, S. I. Abdul Kudus, M. M. Tahir, and M. Z. Hassan ,* Performance Investigation of the UTeM Eco- Car Disc Brake System International Journal of Engineering & Technology IJET-IJENS Vol: 11 No: 06 pp-1-6

[9] R. Limpert, *Brake Design and Safety*. 2nd Edition, Warrendale,Pennsylvania: Society of Automotive Engineering Inc., 1999, pp. 137-144.

[10]. ***ANSYS v.11 user'Manual guide . ANSYS, Inc., Houston, USA; 1996.

[11].*S. B. Sarip,* "Lightweight Friction Brakes for a Road Vehicle with Regenerative Braking," Ph.D. Thesis, Engineering, Design and Technology, Bradford University, 2011.